



Terminal sliding mode control for the trajectory tracking of underactuated Autonomous Underwater Vehicles



Taha Elmokadem^a, Mohamed Zribi^{a,*}, Kamal Youcef-Toumi^b

^a Electrical Engineering Department, Kuwait University, P.O. Box 5969, Safat 13060, Kuwait

^b Department of Mechanical Engineering, Massachusetts Institute of Technology, Cambridge, MA 02139, United States

ARTICLE INFO

Keywords:

AUV
Autonomous Underwater Vehicle
Terminal sliding mode
TSM
Trajectory tracking
Underactuated

ABSTRACT

The aim of this paper is to develop robust control schemes for the lateral motion of underactuated autonomous underwater vehicles (AUVs). The AUV complex dynamics makes their control a challenging task. These challenges include the AUV nonlinear dynamics, unmodeled dynamics, system uncertainties and environmental disturbances. The objective of the proposed control schemes is to solve the trajectory tracking problem of AUVs. These controllers are designed using the concepts of terminal sliding mode control. The control performance of an example AUV (the REMUS AUV), using the proposed control schemes, is evaluated through computer simulations. The simulation results show that the proposed control schemes work well. Moreover, simulation studies are given to evaluate the performance of the proposed control schemes when bounded disturbances are acting on the vehicle. These studies indicate that the proposed control schemes are robust under bounded disturbances.

1. Introduction

In the last decades, autonomous underwater vehicles (AUVs) have been the focus of many oceanic research works due to their emerging applications in many fields. These applications include the exploration of oceans, oceanographic mapping, underwater pipelines inspection, scientific and military missions, and more. These tasks should be performed in an automated way without the interaction of human operators under a variety of load conditions and with unknown sea currents. Therefore, it is necessary to develop robust control schemes that force an AUV to track a desired trajectory to accomplish such hard tasks.

In the literature, the control of AUVs and marine vehicles has been targeted by many researchers. To this end, different control techniques have been used such as sliding mode control (Wang et al., 2012; Yoerger and Slotine, 1985; Healey and Lienard, 1993), higher order sliding mode (Joe et al., 2014), learning control (Yuh, 1994), adaptive control (Qi, 2014; Sahu and Subudhi, 2014; McGann et al., 2008; Antonelli et al., 2003; Do et al., 2004; Li and Lee, 2005), backstepping control (Repoulas and Papadopoulos, 2007), Neural network control (Wang et al., 2014; Yuh, 1990; Fujii and Ura, 1990), fuzzy control (Khaled and Chalhoub, 2013; Wang and Lee, 2003) and suboptimal control (Geranmehr and Nekoo, 2015). However, the control of AUVs continues to be challenging due to the AUV complex dynamics, dynamic effects not known to the controller, system uncertainties

and environmental disturbances. Furthermore, most practical AUVs are underactuated where the available actuators are less than the number of degrees of freedom which adds more challenges to the control design. These challenges along with the wide applications of AUVs generate considerable interest on the control of AUVs and serve as a motivation for this work.

Furthermore, the terminal sliding mode control (TSMC) is used for the design to provide robustness against unmodeled dynamics, model uncertainties and external disturbances due to ocean currents and waves. TSMC is known to be superior over the conventional sliding mode control technique in terms of the finite-time convergence and high steady state tracking precision. It has been used in many works in order to achieve fast and finite-time convergence as well as high precision, for example, see (Feng et al., 2002, 2013; Neila and Tarak, 2011; Zou et al., 2011; Wang and Sun, 2012).

Control schemes were developed to tackle the trajectory tracking problem of AUVs. Some of these schemes have drawbacks in their design such as considering the trajectory tracking problem for some special cases of reference trajectories as in (Ashrafiuon et al., 2008; Lefeber et al., 2003; Pettersen and Nijmeijer, 2001; Jiang, 2002). In Ashrafiuon et al. (2008), a sliding mode controller for the trajectory tracking of surface vessels was proposed that can only track special cases of reference trajectories as will be highlighted later. In Lefeber et al. (2003), Pettersen and Nijmeijer (2001) and Jiang (2002), control

* Corresponding author.

E-mail address: mohamed.zribi@ku.edu.kw (M. Zribi).

laws are developed for the trajectory tracking of underactuated ships using Lyapunov's theory. However, these controllers cannot provide tracking of straight lines because they have restrictions on the rotational motion of the vehicle. Therefore, the main contribution of this work is to develop terminal sliding mode control schemes to solve the trajectory tracking problem of AUVs in the horizontal plane. These developed controllers overcome the drawbacks of the controllers mentioned above by proposing a new design for the AUV's desired velocities that provides tracking for general cases of reference trajectories.

The organization of this paper is as follows. Section 2 presents a model of AUVs for the lateral motion. In Section 3, the problem of the trajectory tracking control of underactuated AUVs is formulated. Section 4 presents the design of the proposed control schemes using the terminal sliding mode concepts. The performance of these controllers are validated using computer simulations, and the results are given in Section 5. Moreover, Section 6 provides simulation studies in order to investigate the robustness of the derived control schemes under bounded disturbances. Section 7 highlights the conclusions of this work.

2. AUV modeling

Following standard practice, modeling an AUV can be treated by handling two parts which are kinematics and kinetics. The kinematics refers to the study of the geometrical aspects of motion while the kinetics deals with the forces causing the motion (Fossen, 2011). In general, the motion of an AUV involves 6 degrees of freedom (DOFs). These DOFs correspond to the set of independent displacements and rotations which determine the position and orientation of the vehicle, and they are referred to as the surge (longitudinal motion), the sway (lateral motion), the heave (vertical motion), the roll (rotational motion about the longitudinal axis), the pitch (rotational motion about the lateral axis) and the yaw (rotation about the vertical axis) (Fossen, 2002).

In this study, only the motion in the horizontal plane (lateral dynamics) of the AUV is considered which includes the surge, the sway and the yaw. The model for the lateral motion of an AUV can be developed using two special reference frames. These frames are the *Earth-fixed* $\{n\}$ reference frame, which is considered to be inertial and its origin is fixed, and the *body-fixed* $\{b\}$ reference frame, which is a moving frame fixed to the vehicle, as depicted in Fig. 1. The origin of the body-fixed frame is defined usually to coincide with the vehicle's center of mass, and the axes of this frame are chosen along the vehicle's principle axes of inertia.

A complete modeling of AUVs is derived and presented in Fossen (2002) as well as standard models for horizontal and longitudinal motions. The model of the horizontal motion of AUVs is the one considered in this work. The kinematic equations of this model are such that:

$$\dot{x} = u \cos \psi - v \sin \psi \dot{\psi} = u \sin \psi + v \cos \psi \dot{\psi} = r \quad (1)$$

where u and v are the surge and the sway linear velocities of the AUV respectively, r is the yaw angular velocity of the AUV, x and y express

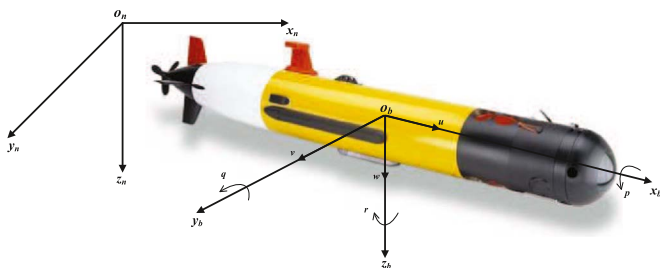


Fig. 1. The earth-fixed and body-fixed reference frames for an AUV.

the coordinates of the vehicle's center of mass, and ψ describes the orientation of the vehicle. The position and orientation of the AUV (i.e. (x, y, ψ)) are defined in the earth-fixed frame $\{n\}$ while the linear and angular velocities (i.e. (u, v, r)) are defined in the body-fixed frame $\{b\}$.

Consider the following notation: m is the mass of the AUV, I_z is the vehicle's moment of inertia about the z -axis, X_u , Y_v and N_r are negative terms that include the effects of linear damping, and $X_{\dot{u}}$, $Y_{\dot{v}}$ and $N_{\dot{r}}$ are the hydrodynamic added mass terms in the surge, the sway and the yaw directions of motion respectively. By neglecting the heave, roll and pitch motions, the lateral dynamics of an AUV can be represented by:

$$\ddot{u} = M_1(X_u u + a_{23}vr + \tau_u)\dot{v} = M_2(Y_v v + a_{13}ur)\dot{r} = M_3(N_r r + a_{12}uv + \tau_r) \quad (2)$$

where $M_1 := 1/(m - X_{\dot{u}})$, $M_2 := 1/(m - Y_{\dot{v}})$, $M_3 := 1/(I_z - N_{\dot{r}})$, $a_{12} := Y_{\dot{v}} - X_{\dot{u}}$, $a_{13} := X_{\dot{u}} - m$ and $a_{23} := m - Y_{\dot{v}}$. The control inputs are the surge force τ_u and the yaw moment τ_r , generated by the actuators.

Clearly, the control problem of the AUV model represented by (1) and (2) is considered to be underactuated since actuation forces and moments are generated in the surge and yaw directions only while the sway motion is unactuated.

3. Problem formulation

3.1. Trajectory tracking error coordinates

In order to formulate the trajectory tracking control problem investigated in this work, consider the model of the AUV for the lateral motion given by (1) and (2). Define the following position tracking errors,

$$x_e = x - x_d, y_e = y - y_d \quad (3)$$

where x_d and y_d are the coordinates of the desired, time-varying position. The position error dynamics can be obtained by taking the time derivatives of the position errors in (3), and using (1), as follows:

$$\begin{bmatrix} \dot{x}_e \\ \dot{y}_e \end{bmatrix} = \begin{bmatrix} \cos \psi & -\sin \psi \\ \sin \psi & \cos \psi \end{bmatrix} \begin{bmatrix} u \\ v \end{bmatrix} - \begin{bmatrix} \dot{x}_d \\ \dot{y}_d \end{bmatrix} \quad (4)$$

Also, let the velocity tracking errors be such that:

$$e_u = u - u_d, e_v = v - v_d \quad (5)$$

where u_d and v_d are the desired surge and sway velocities respectively. Taking the time derivative of (5), and using (2), yields the following,

$$\dot{e}_u = M_1(X_u u + a_{26}vr + \tau_u) - \dot{u}_d, \dot{e}_v = M_2(Y_v v + a_{16}ur) - \dot{v}_d \quad (6)$$

3.2. Problem formulation

The trajectory tracking control problem of AUVs refers to the design of control laws so that the vehicle's position (x, y) tracks a desired, time-varying position (x_d, y_d) . Fig. 2 shows a block diagram representation of the control problem considered in this work for the AUV trajectory tracking. The formulation of this control problem is such that:

For the AUV model in the horizontal plane described by (1) and (2), derive a control law that computes the applied surge force τ_u and the yaw moment τ_r , so that the vehicle's actual position $(x(t), y(t))$ tracks a desired, time-varying trajectory $(x_d(t), y_d(t))$.

4. Control design

4.1. Control design overview

In this section, the proposed control schemes for the trajectory tracking control problem of AUVs are presented. The design is divided into two parts to reduce the complexity of the overall analysis. In the first part, the surge and sway velocities are designed on the kinematic

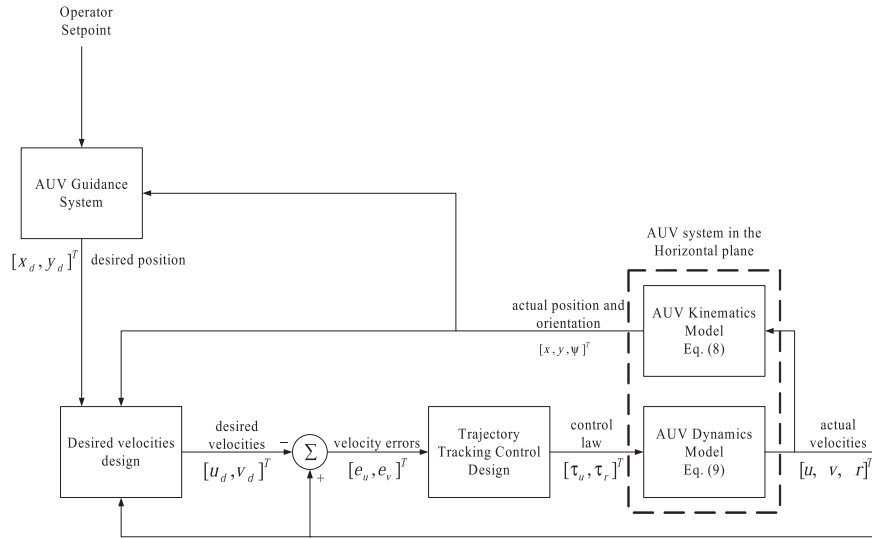


Fig. 2. A block diagram of the AUV's trajectory tracking control problem using terminal sliding mode concepts.

level to ensure the convergence of the vehicle's position tracking errors to zero. The second part deals with the dynamics of the vehicle in order to guarantee the convergence of the velocities of the AUV to the desired ones designed in the first part. This is done using the terminal sliding mode concepts given in Appendix A. Furthermore, an analysis is made in order to ensure that the yaw velocity remains bounded under the application of the proposed controllers.

The work presented in Ashrafiun et al. (2008), where a controller for the trajectory tracking of surface vessels is designed using the sliding mode control techniques, is considered for the design of the desired velocities. The control scheme developed by Ashrafiun has some drawbacks, which are highlighted in Yu et al. (2012), since the desired surge and sway velocities are chosen in terms of the time derivatives of the reference position as follows:

$$u_d = \dot{x}_d \cos \psi + \dot{y}_d \sin \psi, \quad v_d = -\dot{x}_d \sin \psi + \dot{y}_d \cos \psi \quad (7)$$

This design of the desired velocities solves the trajectory tracking control problem for special cases. This can be shown by considering the following general form of reference trajectories:

$$x_d = a(t) + C_1, \quad y_d = b(t) + C_2, \quad (8)$$

where C_1 and C_2 are constants, and $a(t)$ and $b(t)$ are differentiable time-varying functions.

Since the desired velocities in (7) depend only on the derivatives of the reference trajectories \dot{x}_d and \dot{y}_d , it is clear that the constant parameters C_1 and C_2 in (8) have no effect on the desired velocities. Thus, the control scheme developed in Ashrafiun et al. (2008) is valid only for special cases of the reference trajectories with appropriate values of C_1 and C_2 . In this work, a different design for the desired velocities is proposed in order to overcome this problem taking into account the work proposed in Martins (2008).

Moreover, the proposed control schemes in this paper are designed using the terminal sliding mode control technique. This technique is superior over the conventional sliding mode method since it provides finite-time convergence and steady state error improvement.

It should be mentioned that, the derived control schemes in this section are based on the following assumptions:

- all the states are measurable and are available for feedback,
- the vehicle is moving forward (i.e. $u_d > 0$).

4.2. Desired velocities design

Proposition 1. Let the desired surge and sway velocities be as

follows:

$$\begin{bmatrix} u_d \\ v_d \end{bmatrix} = \begin{bmatrix} \cos \psi & \sin \psi \\ -\sin \psi & \cos \psi \end{bmatrix} \begin{bmatrix} \dot{x}_d + l_x \tanh\left(-\frac{k_x}{l_x} x_e\right) \\ \dot{y}_d + l_y \tanh\left(-\frac{k_y}{l_y} y_e\right) \end{bmatrix} \quad (9)$$

where $k_x, k_y > 0$ and $l_x, l_y \neq 0$. It is guaranteed that the position tracking errors defined in (3) will asymptotically converge to zero if the velocity tracking errors in (5) converge to zero.

Proof. Eq. (1) leads to the following equation:

$$\begin{bmatrix} u \\ v \end{bmatrix} = \begin{bmatrix} \cos \psi & \sin \psi \\ -\sin \psi & \cos \psi \end{bmatrix} \begin{bmatrix} \dot{x} \\ \dot{y} \end{bmatrix} \quad (10)$$

Substituting (9) and (10) into (5) yields the following:

$$\begin{bmatrix} e_u \\ e_v \end{bmatrix} = \bar{R}_h \begin{bmatrix} \dot{x}_e - l_x \tanh\left(-\frac{k_x}{l_x} x_e\right) \\ \dot{y}_e - l_y \tanh\left(-\frac{k_y}{l_y} y_e\right) \end{bmatrix} \quad (11)$$

where

$$\bar{R}_h = \begin{bmatrix} \cos \psi & \sin \psi \\ -\sin \psi & \cos \psi \end{bmatrix}.$$

It is clear that $|\bar{R}_h| = 1$ which indicates that the matrix \bar{R}_h is non-singular. Therefore, according to (11), the convergence of the velocity errors e_u and e_v to zero guarantee the following,

$$\dot{x}_e = l_x \tanh\left(-\frac{k_x}{l_x} x_e\right), \quad \dot{y}_e = l_y \tanh\left(-\frac{k_y}{l_y} y_e\right). \quad (12)$$

Furthermore, consider the following Lyapunov function candidate:

$$V_1 = \frac{1}{2} x_e^2 + \frac{1}{2} y_e^2. \quad (13)$$

The time derivative of this Lyapunov function along the dynamics in (12) is such that:

$$\dot{V}_1 = x_e \dot{x}_e + y_e \dot{y}_e = -l_x x_e \tanh\left(\frac{k_x}{l_x} x_e\right) - l_y y_e \tanh\left(\frac{k_y}{l_y} y_e\right) \quad (14)$$

It is evident from (14) that $\dot{V}_1 < 0$ for $(x_e, y_e) \neq (0, 0)$ since $k_x, k_y > 0$ and $l_x, l_y \neq 0$. Therefore, it is guaranteed that (x_e, y_e) asymptotically converge to $(0, 0)$.

Thus, it can be concluded that the convergence of the vehicle's surge and sway velocities to the desired velocities proposed in (9) ensures the asymptotic convergence of the position tracking errors (x_e, y_e) to

(0, 0), □.

In order to proceed with the control design, The time derivatives of the proposed desired velocities in (9) are obtained first as follows,

$$\begin{bmatrix} \dot{u}_d \\ \dot{v}_d \end{bmatrix} = r \begin{bmatrix} v_d \\ -u_d \end{bmatrix} + \begin{bmatrix} \cos \psi & \sin \psi \\ -\sin \psi & \cos \psi \end{bmatrix} \begin{bmatrix} \ddot{x}_d - k_x \dot{x}_e \operatorname{sech}^2\left(-\frac{k_x}{l_x} x_e\right) \\ \ddot{y}_d - k_y \dot{y}_e \operatorname{sech}^2\left(-\frac{k_y}{l_y} y_e\right) \end{bmatrix} \quad (15)$$

Also, the second derivative of the desired sway velocity with respect to time is obtained as follows,

$$\ddot{v}_d = \dot{\Gamma} - u_d \dot{r} \quad (16)$$

where Γ is defined such that,

$$\begin{aligned} \Gamma &= -\ddot{x}_d \sin \psi + \ddot{y}_d \cos \psi - \ddot{x}_d r \cos \psi - \ddot{y}_d r \sin \psi - \dot{u}_d r + Y_1 r \cos \psi \\ &\quad + Y_2 r \sin \psi + \dot{Y}_1 \sin \psi - \dot{Y}_2 \cos \psi Y_1 = k_x \dot{x}_e \operatorname{sech}^2\left(-\frac{k_x}{l_x} x_e\right) Y_2 \\ &= k_y \dot{y}_e \operatorname{sech}^2\left(-\frac{k_y}{l_y} y_e\right). \end{aligned} \quad (17)$$

The parameters in (17) will be used in the control design. Notice that these parameters depends on the desired position, velocity, acceleration and jerk. Therefore, it is required from the AUV's guidance system to provide them. For complex paths, path planning algorithms that minimizes the jerk will be more suitable in order to avoid problems in practical implementations. Many researchers have developed minimum jerk trajectory planners in the literature.

4.3. Terminal sliding mode controller (TSMC)

Let the TSM surfaces be chosen in terms of the surge and sway velocity errors such that:

$$S_1 = e_u + \beta_1 (\tilde{e}_u)^{q_1/p_1} \quad (18)$$

$$S_2 = \dot{e}_v + \beta_2 (e_v)^{q_2/p_2} \quad (19)$$

where $\beta_1, \beta_2 > 0$, p_i and q_i are positive odd integers such that $p_i > q_i$ for $i=1,2$.

By differentiating the proposed TSM surfaces in (18) and (19) along the error dynamics in (6) and using (16), one can obtain

$$\dot{S}_1 = M_1(X_u u + a_{26} v r + \tau_u) - \dot{u}_d + \beta_1 \left(\frac{q_1}{p_1}\right) e_u (\tilde{e}_u)^{q_1/p_1-1} \quad (20)$$

$$\begin{aligned} \dot{S}_2 &= M_2(Y_v \dot{v} + a_{16} \dot{u} r) - \Gamma + M_6(M_2 a_{16} u + u_d)(N_r r + a_{12} u v + \tau_r) \\ &\quad + \beta_2 \left(\frac{q_2}{p_2}\right) \dot{e}_v (e_v)^{q_2/p_2-1} \end{aligned} \quad (21)$$

In order to ensure the finite-time convergence to zero of the proposed sliding surfaces, we impose the following dynamics:

$$\dot{S}_1 = -W_1 \operatorname{sign}(S_1) \quad (22)$$

$$\dot{S}_2 = -W_2 \operatorname{sign}(S_2) \quad (23)$$

where W_1 and W_2 are positive design parameters.

The required surge and yaw control laws are obtained as follows:

$$\tau_u = -X_u u - a_{26} v r + \frac{1}{M_1} \left(\dot{u}_d - \beta_1 \frac{q_1}{p_1} e_u (\tilde{e}_u)^{\frac{q_1}{p_1}-1} \right) + \frac{1}{M_1} (-W_1 \operatorname{sign}(S_1)) \quad (24)$$

$$\begin{aligned} \tau_r &= -N_r r - a_{12} u v + \frac{1}{M_6(M_2 a_{16} u + u_d)} \left(M_2(-Y_v \dot{v} - a_{16} \dot{u} r) + \Gamma \right. \\ &\quad \left. - \beta_2 \frac{q_2}{p_2} \dot{e}_v (e_v)^{\frac{q_2}{p_2}-1} - W_2 \operatorname{sign}(S_2) \right) \end{aligned} \quad (25)$$

where Γ is defined in (17).

Theorem 2. Consider the model of the AUV's lateral motion expressed by (1) and (2). Let the surge and sway controllers be chosen as in (24) and (25), then the surge and sway velocities will converge to their desired values in finite time. Furthermore, the position tracking errors (x_e, y_e) will converge to (0, 0) while the yaw motion remains bounded.

Proof. Choose the following Lyapunov function candidate:

$$V_1 = \frac{1}{2} S_1^2 + \frac{1}{2} S_2^2 \quad (26)$$

By using (20) and (21), the time derivative of the proposed Lyapunov function is such that:

$$\begin{aligned} \dot{V}_1 &= S_1 \dot{S}_1 + S_2 \dot{S}_2 = S_1 \left(M_1(X_u u + a_{26} v r + \tau_u) - \dot{u}_d + \beta_1 \left(\frac{q_1}{p_1}\right) e_u (\tilde{e}_u)^{q_1/p_1-1} \right) \\ &\quad + S_2 \left(M_2(Y_v \dot{v} + a_{16} \dot{u} r) - \Gamma + M_6(M_2 a_{16} u + u_d)(N_r r + a_{12} u v + \tau_r) + \right. \\ &\quad \left. \beta_2 \left(\frac{q_2}{p_2}\right) \dot{e}_v (e_v)^{q_2/p_2-1} \right) \end{aligned} \quad (27)$$

Substituting for the control laws (24) and (25) into (27) yields,

$$\dot{V}_1 = -W_1 S_1 \operatorname{sign}(S_1) - W_2 S_2 \operatorname{sign}(S_2) = -W_1 |S_1| - W_2 |S_2| \quad (28)$$

Therefore, since $W_1, W_2 > 0$, \dot{V}_1 is negative definite. This implies that the system's trajectories will exhibit a finite time reachability to the sliding surfaces defined in (18) and (19) from any initial condition. Once the trajectories are on the sliding surfaces $S_1 = S_2 = 0$, the following dynamics are obtained

$$e_u + \beta_1 (\tilde{e}_u)^{q_1/p_1} = 0 \quad \dot{e}_v + \beta_2 (e_v)^{q_2/p_2} = 0$$

Using Lemma 1, these dynamics guarantees the finite-time convergence of the velocity tracking errors (e_u, e_v) to (0, 0). Thus, the velocities will reach the desired values defined by (9) which will guarantee the convergence of the position tracking errors (x_e, y_e) to (0, 0) according to Proposition 1.

Also, the sway dynamics will be such that:

$$\dot{v}_d = M_2(Y_v v_d + a_{16} u_d r) \quad (29)$$

Substituting for \dot{v}_d from (15), one can get,

$$\begin{aligned} &-\left(\ddot{x}_d - k_x \dot{x}_e \operatorname{sech}^2\left(-\frac{k_x}{l_x} x_e\right) \right) \sin \psi + \left(\ddot{y}_d - k_y \dot{y}_e \operatorname{sech}^2\left(-\frac{k_y}{l_y} y_e\right) \right) \cos \psi \\ &= M_2 Y_v v_d + (1 + M_2 a_{16}) u_d r \end{aligned} \quad (30)$$

Since $u_d > 0$, and from (9) and (12), it is clear that u_d, v_d, \dot{x}_e and \dot{y}_e are bounded. Therefore it can be concluded that r will remain bounded.

Moreover, choose the following Lyapunov function candidate:

$$V_2 = \frac{1}{2} r^2 \quad (31)$$

By differentiating with respect to time, one can get

$$\dot{V}_2 = r \dot{r} = M_6 r (N_r r + a_{12} u v + \tau_r) = M_6 N_r r^2 + M_6 (a_{12} u v + \tau_r) r$$

Since $N_r < 0$ (N_r is a damping term) and $M_6 > 0$, $\dot{V}_2 < 0$ for:

$$|N_r r| > |a_{12} u v + \tau_r| \quad (32)$$

In addition, $\dot{V}_2 < 0$ indicates $|r|$ is decreasing in the set $|r| > |a_{12} u v + \tau_r|/|N_r|$. □

4.4. Fast terminal sliding mode controller (FTSMC)

For the FTSM controller design, let $\alpha_1, \alpha_2, \beta_1$ and β_2 be positive constants, and p_i and q_i be positive odd integers such that $p_i > q_i$ for $i=1,2$. Define the following sliding surfaces:

Table 1
The REMUS AUV model parameters.

Parameter	Value	Units
m	30.48	kg
I_x	3.45	kg·m ²
X_u	-8.8065	kg/s
Y_v	-65.5457	kg/s
N_r	-6.7352	kg/s
$X_{\dot{u}}$	-0.93	kg
$Y_{\dot{v}}$	-35.5	kg
$N_{\dot{r}}$	-35.5	kg·m ²

$$S_1 = e_u + \alpha_1 \tilde{e}_u + \beta_1 (\tilde{e}_u)^{q_1/p_1} \quad (33)$$

$$S_2 = \dot{e}_v + \alpha_2 e_v + \beta_2 (e_v)^{q_2/p_2}. \quad (34)$$

Also, let Γ be defined as in (17), and W_1 and W_2 be positive scalars.

Theorem 3. The FTSM control law:

$$\tau_u = -X_u u - a_{26} v r + \frac{1}{M_1} \left(\dot{u}_d - \alpha_1 e_u - \beta_1 \frac{q_1}{p_1} e_u (\tilde{e}_u)^{\frac{q_1}{p_1}-1} \right) + \frac{1}{M_1} (-W_1 \text{sign}(S_1)) \quad (35)$$

$$\tau_r = -N_r r - a_{12} u v + \frac{1}{M_6 (M_2 a_{16} u + u_d)} \left(M_2 (-Y_v \dot{v} - a_{16} \dot{u} r) + \Gamma - \alpha_2 \dot{e}_v - \beta_2 \frac{q_2}{p_2} \dot{e}_v (e_v)^{\frac{q_2}{p_2}-1} - W_2 \text{sign}(S_2) \right) \quad (36)$$

when applied to an AUV moving in the horizontal plane with the desired velocities chosen as in (9) guarantees the asymptotic convergence of the position tracking errors (x_e, y_e) to $(0, 0)$ while maintaining the boundedness of the yaw motion.

Proof. Taking the time derivative of the surfaces S_1 and S_2 in (33) and (34) along the error dynamics in (6) and using the control laws given by (35) and (36), we obtain the following:

$$\begin{aligned} \dot{S}_1 &= \dot{e}_u + \alpha_1 \dot{e}_u + \beta_1 \left(\frac{q_1}{p_1} \right) e_u (\tilde{e}_u)^{q_1/p_1-1} = M_1 (X_u u + a_{26} v r + \tau_u) - \dot{u}_d + \alpha_1 e_u \\ &\quad + \beta_1 \left(\frac{q_1}{p_1} \right) e_u (\tilde{e}_u)^{q_1/p_1-1} = -W_1 \text{sign}(S_1) \end{aligned} \quad (37)$$

$$\begin{aligned} \dot{S}_2 &= \ddot{e}_v + \alpha_2 \dot{e}_v + \beta_2 \left(\frac{q_2}{p_2} \right) \dot{e}_v (e_v)^{q_2/p_2-1} = M_2 (Y_v \dot{v} + a_{16} \dot{u} r) - \Gamma \\ &\quad + M_6 (M_2 a_{16} u + u_d) (N_r r + a_{12} u v + \tau_r) + \alpha_2 \dot{e}_v + \beta_2 \left(\frac{q_2}{p_2} \right) \dot{e}_v (e_v)^{q_2/p_2-1} \\ &= -W_2 \text{sign}(S_2) \end{aligned} \quad (38)$$

Now, let the Lyapunov function candidate V_3 be such that:

$$V_3 = \frac{1}{2} S_1^2 + \frac{1}{2} S_2^2 \quad (39)$$

Differentiating V_3 with respect to time and using (37) and (38) yields:

$$\dot{V}_3 = S_1 \dot{S}_1 + S_2 \dot{S}_2 = -W_1 S_1 \text{sign}(S_1) - W_2 S_2 \text{sign}(S_2) = -W_1 |S_1| - W_2 |S_2| \quad (40)$$

It is clear from (40) that $\dot{V}_3 < 0$ for $(S_1, S_2) \neq (0, 0)$. Therefore, the surfaces S_1 and S_2 will reach zero in finite time from any given initial conditions provided that the design parameters W_1 and W_2 are chosen to be positive constants. Once the trajectories are on the sliding surfaces, the following dynamics are guaranteed:

$$e_u + \alpha_1 \tilde{e}_u + \beta_1 (\tilde{e}_u)^{q_1/p_1} = 0 \quad (41)$$

$$\dot{e}_v + \alpha_2 e_v + \beta_2 (e_v)^{q_2/p_2} = 0. \quad (42)$$

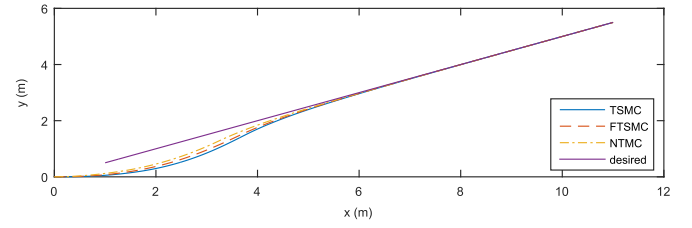


Fig. 3. The actual and desired paths of the AUV using the proposed control schemes.

According to Lemma 2, these dynamics ensure the finite-time convergence of (e_u, e_v, \dot{e}_v) to $(0, 0, 0)$. Furthermore, since the desired velocities are chosen as in (9), the position tracking errors (x_e, y_e) will converge to $(0, 0)$ based on Proposition 1.

Also, the sway dynamics will be such that:

$$\dot{v}_d = M_2 (Y_v v_d + a_{16} u_d r) \quad (43)$$

Since $u_d > 0$, and u_d, v_d and \dot{v}_d are bounded, it is clear that r will remain bounded. □

4.5. Non-singular terminal sliding mode controller (NTSMC)

The proposed TSM and FTSM controllers presented in the previous subsections may exhibit an unbounded behavior for the case of $\dot{\mu} \neq 0$ when $\mu = 0$ before the trajectories reach the sliding surfaces $S_i = 0$ ($i=1,2$) where $\mu = \tilde{e}_u, e_v$. Even after the sliding surface is reached, the singularity may occur since the trajectories are not guaranteed to stay on the sliding surface due to computation errors and uncertain factors especially near the equilibrium point $(\mu, \mu) = (0, 0)$; the singularity due to the case $\dot{\mu} \neq 0$ when $\mu = 0$ may occur occasionally. Therefore, to overcome this singularity problem, a non-singular terminal sliding mode (NTSM) controller is proposed in this section motivated by the work presented in (Feng et al., 2002).

Define the non-singular sliding surfaces in terms of the velocity tracking errors such that:

$$S_1 = \tilde{e}_u + c_1 (e_u)^{p_1/q_1} \quad (44)$$

$$S_2 = e_v + c_2 (\dot{e}_v)^{p_2/q_2} \quad (45)$$

where $c_1, c_2 > 0$, p_i and q_i are odd positive integers satisfying $p_i > q_i$ for $i=1,2$.

Differentiating (44) and (45) with respect to time and using Eqs. (2), (5) and (16), we obtain

$$\dot{S}_1 = \dot{e}_u + c_1 \frac{p_1}{q_1} \dot{e}_u (e_u)^{\frac{p_1}{q_1}-1} = \dot{e}_u + c_1 \frac{p_1}{q_1} (M_1 (X_u u + a_{26} v r + \tau_u) - \dot{u}_d) (e_u)^{\frac{p_1}{q_1}-1} \quad (46)$$

$$\begin{aligned} \dot{S}_2 &= \dot{e}_v + c_2 \frac{p_2}{q_2} \dot{e}_v (\dot{e}_v)^{p_2/q_2-1} = \dot{e}_v + c_2 \frac{p_2}{q_2} (\dot{e}_v)^{p_2/q_2-1} (M_2 (Y_v \dot{v} + a_{16} \dot{u} r) - \Gamma \\ &\quad + M_6 (M_2 a_{16} u + u_d) (N_r r + a_{12} u v + \tau_r)) \end{aligned} \quad (47)$$

We propose the following NTSM controllers:

$$\tau_u = -X_u u - a_{26} v r + \frac{\dot{u}_d}{M_1} - \frac{1}{c_1} \frac{q_1}{p_1} \frac{1}{M_1} (e_u)^{2-\frac{p_1}{q_1}} - \frac{W_1}{M_1} \text{sign}(S_1) \quad (48)$$

$$\begin{aligned} \tau_r &= -N_r r - a_{12} u v + \frac{1}{M_6 (M_2 a_{16} u + u_d)} \left(M_2 (-Y_v \dot{v} - a_{16} \dot{u} r) + \Gamma \right. \\ &\quad \left. - \frac{1}{c_2} \frac{q_2}{p_2} (\dot{e}_v)^{2-\frac{p_2}{q_2}} - W_2 \text{sign}(S_2) \right) \end{aligned} \quad (49)$$

where $W_1, W_2 > 0$ and Γ is defined as in (17).

Theorem 4. The NTSM control laws (48)-(49) with the desired velocities given by (9) when applied to the AUV model moving in the horizontal plane guarantee the asymptotic convergence to zero of the

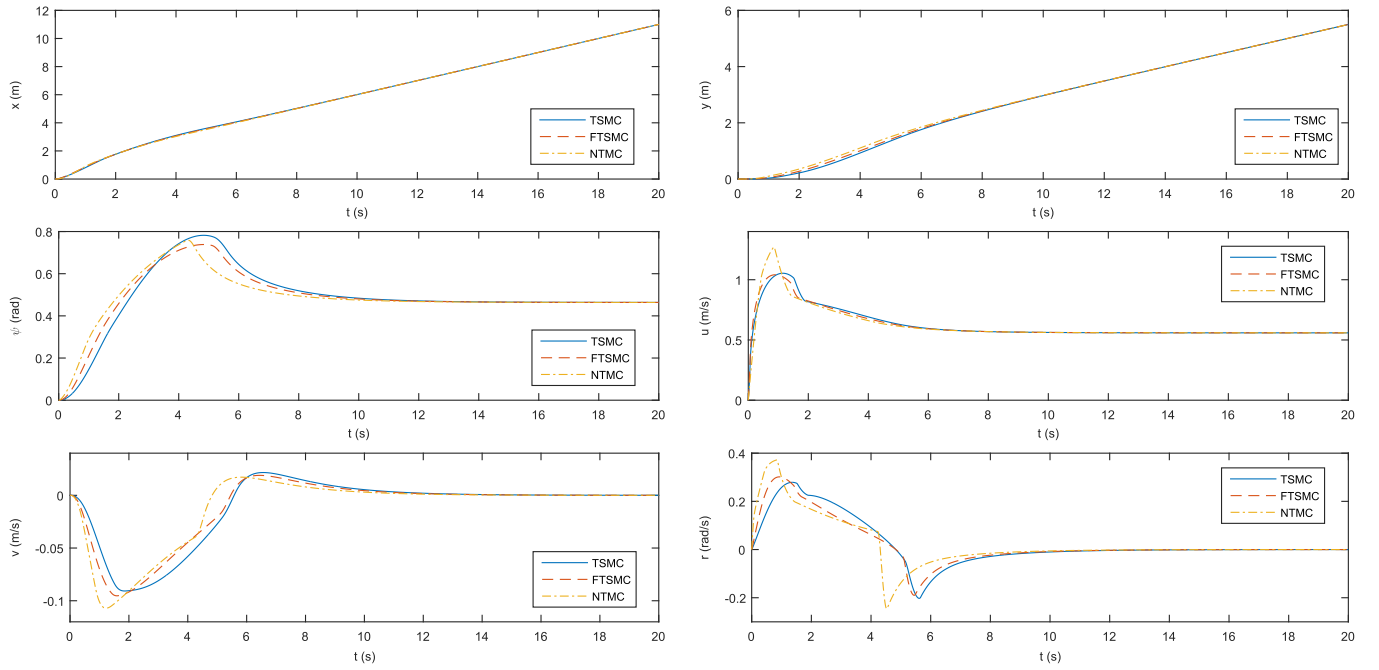


Fig. 4. The positions, the orientation and the velocities of the AUV versus time using the proposed control schemes.

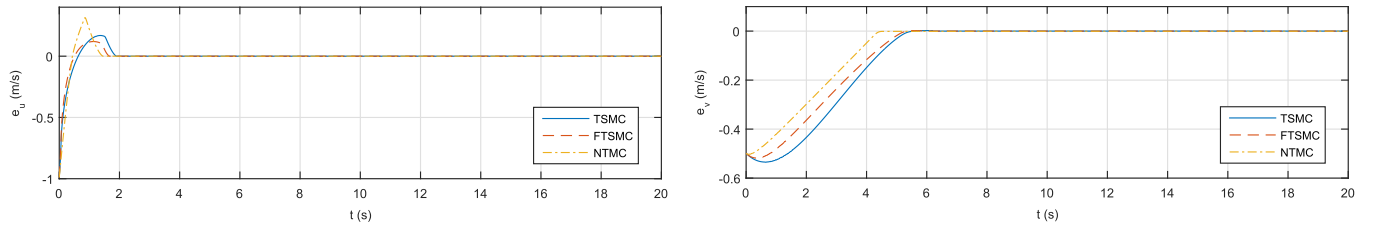


Fig. 5. The velocity tracking errors of the AUV versus time using the proposed control schemes.

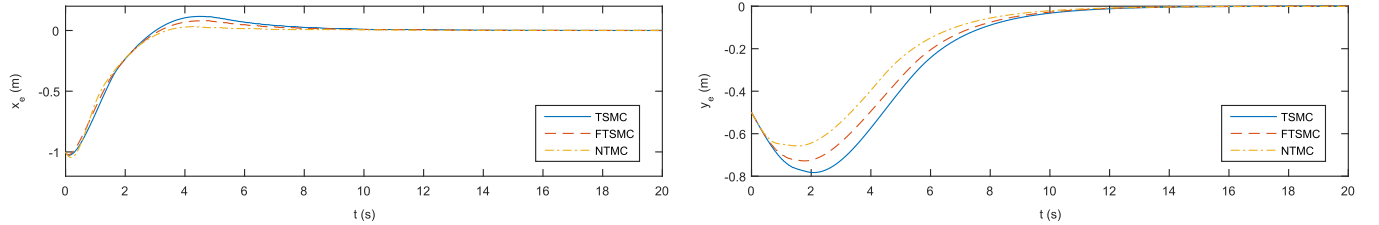


Fig. 6. The position tracking errors of the AUV versus time using the proposed control schemes.

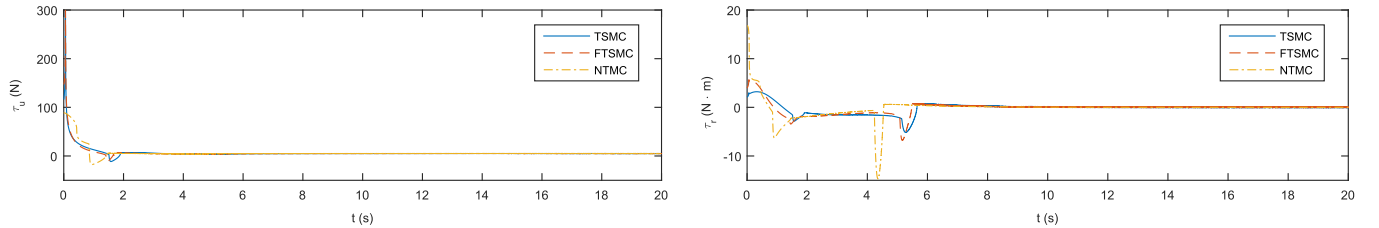


Fig. 7. The surge and yaw controllers of the AUV versus time using the proposed control schemes.

position tracking errors (x_e , y_e) while maintaining the boundedness of the yaw motion of the AUV.

Proof. Consider the Lyapunov function candidate V_4 such that,

$$V_4 = \frac{1}{2}S_1^2 + \frac{1}{2}S_2^2 \quad (50)$$

The time derivative of V_4 is obtained using (46) and (47) such that,

$$\begin{aligned} \dot{V}_4 = & S_1 \dot{S}_1 + S_2 \dot{S}_2 = S_1 \left[e_u + c_1 \frac{p_1}{q_1} (M_1(X_u u + a_{26}vr + \tau_u) - \dot{u}_d)(e_u)^{\frac{p_1}{q_1}-1} \right] \\ & + S_2 \left[\dot{e}_v + c_2 \frac{p_2}{q_2} (e_v)^{p_2/q_2-1} (M_2(Y_v \dot{v} + a_{16}\dot{u}r) - \Gamma + M_6(M_2 a_{16}u + u_d)(N_r r + a_{12}uv + \tau_r)) \right] \end{aligned} \quad (51)$$

Using (48) and (49) to substitute for the control laws in \dot{V}_4 gives the following,

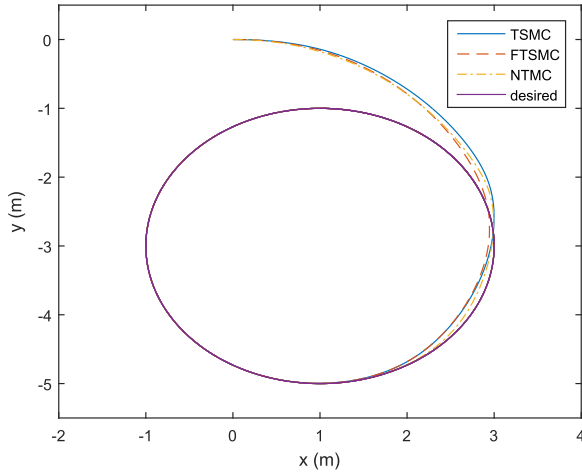


Fig. 8. The actual and desired paths of the AUV using the proposed control schemes for a circular path.

$$\dot{V}_4 = -W_1 c_1 \frac{p_1}{q_1} (e_u)^{\frac{p_1}{q_1}-1} S_1 \text{sign}(S_1) - W_2 c_2 \frac{p_2}{q_2} (\dot{e}_v)^{\frac{p_2}{q_2}-1} S_2 \text{sign}(S_2) \quad (52)$$

One can define the following:

$$\rho_1(e_u) = c_1 \frac{p_1}{q_1} (e_u)^{\frac{p_1}{q_1}-1} \quad (53)$$

$$\rho_2(\dot{e}_v) = c_2 \frac{p_2}{q_2} (\dot{e}_v)^{\frac{p_2}{q_2}-1} \quad (54)$$

It is obvious that $\rho_i > 0$ for $i=1,2$ since (i) $c_i, p_i, q_i > 0$ and (ii) p_i and q_i are odd integers such that $p_i > q_i$ which implies that $p_i - q_i$ is even. Hence, \dot{V}_4 can be written as:

$$\dot{V}_4 = -W_1 \rho_1(e_u) |S_1| - W_2 \rho_2(\dot{e}_v) |S_2| \quad (55)$$

Clearly, \dot{V}_4 is negative definite provided that $W_1, W_2 > 0$. Therefore, the finite-time convergence of both surfaces S_1 and S_2 to zero is guaranteed. Hence, the trajectories will reach the sliding surfaces $S_1 = S_2 = 0$. On the sliding surfaces, the following dynamics are imposed:

$$\ddot{e}_u + c_1 (e_u)^{p_1/q_1} = 0 \quad (56)$$

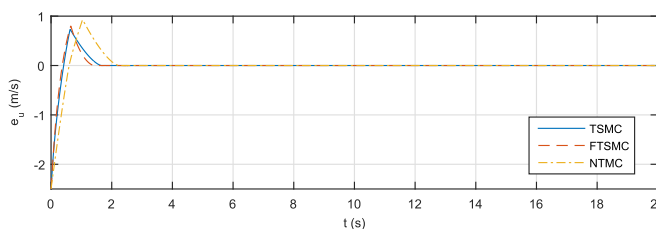
$$e_v + c_2 (\dot{e}_v)^{p_2/q_2} = 0 \quad (57)$$

The dynamics in (56) and (57) are equivalent to those for the conventional TSM when $S=0$ where S is given by (A.2). Hence, according to Lemma 1, the finite-time convergence of (e_u, e_v, \dot{e}_v) to $(0, 0, 0)$ is ensured. That is, the AUV's velocities will converge to their desired values associated with (9) in finite time which will guarantee the convergence of the position tracking errors (x_e, y_e) to $(0, 0)$ based on Proposition 1.

Moreover, the sway dynamics will be such that:

$$\dot{v}_d = M_2(Y_v v_d + a_{16} u_d r) \quad (58)$$

which implies that r will remain bounded since u_d, v_d and \dot{v}_d are bounded, and $u_d > 0$. \square



Remark 1. In order to avoid the well known chattering problem, the discontinuous sign function used in the proposed control laws can be replaced by using the popular boundary layer concept. Generally, the boundary layer is defined by replacing $\text{sign}(S)$ in the control laws by a saturating function $\text{sat}(S)$ defined as follows:

$$\text{sat}(S) = \begin{cases} -1, & S < -\varphi \\ S/\varphi, & -\varphi \leq S \leq \varphi \\ 1, & S > \varphi \end{cases} \quad (59)$$

where φ is a constant that normally describes the error associated with the smooth approximation of the sign function by the saturation function, and the boundary layer thickness is defined as 2φ .

The choice of the function $\text{sat}(S)$ given in (59) does not affect the convergence results obtained in this section. Recall that the proposed controllers force the following dynamics: $\dot{S} = -W \text{sign}(S)$. By considering the Lyapunov function candidate $\bar{V} = \frac{1}{2} S^2$ and replacing $\text{sign}(S)$ with $\text{sat}(S)$, we get $\dot{\bar{V}} = -W \text{sat}(S)$. It is clear from (59) that the condition $\dot{\bar{V}} < 0$ is always satisfied since $\dot{\bar{V}} = -W|S| < 0$ if $|S| > \varphi$, and $\dot{\bar{V}} = -\frac{W}{\varphi} S^2 < 0$ if $|S| < \varphi$.

It should be noted that the designed controllers using this approximation drive the system states to a neighborhood of the sliding surface, and the ideal sliding no longer takes place. However, this difference can be negligible by adjusting the width of the boundary layer 2φ to make it small (Khan, 2003). This approximation is compared with other approximations for chattering reduction using experimental results in (De Jager, 1992).

Remark 2. The designed control schemes in (24) and (25), (35) and (36), and (48) and (49) can be computed easily as long as the AUV's guidance system provide the control system with the information of the desired path. This makes these schemes to be easy to implement which is one of the main features of the sliding mode control technique.

5. Simulation results

The proposed control schemes are applied to the model of lateral dynamics for an example AUV which is described by the kinematic and dynamic equations of motion in (1) and (2) respectively. Computer simulations are performed considering the REMUS AUV; the model parameters of this vehicle are presented in Table 1. In these simulations, the initial states are taken to be zero (i.e. the vehicle is at rest) such that: $x(0) = y(0) = \psi(0) = u(0) = v(0) = r(0) = 0$. Also, the initial values of errors integrals are taken such that $\tilde{e}_u(0) = 0.05$ and $\tilde{e}_v(0) = 0$.

The performance of the system is tested under the proposed controllers using reference trajectories with the following choice:

$$x_d(t) = 0.5t + 1 \text{ m}, \quad y_d(t) = 0.25t + 0.5 \text{ m}.$$

The boundary layer approximation presented in (59) is used to approximate the sign function in the proposed controllers to reduce the chattering phenomena. The simulations are carried out using the following design parameters: $l_x = l_y = 2$, $k_x = k_y = 0.5$, $\varphi = 0.01$, and the design parameters for each control scheme are selected as follows,

- TSMC: $\beta_1 = 1.5$, $\beta_2 = 1$, $q_1/p_1 = q_2/p_2 = 3/5$, $W_1 = 0.5$ and $W_2 = 0.15$.
- FTSMC: $\alpha_1 = \alpha_2 = 1$, $\beta_1 = 1.5$, $\beta_2 = 1$, $q_1/p_1 = q_2/p_2 = 3/5$, $W_1 = 0.5$

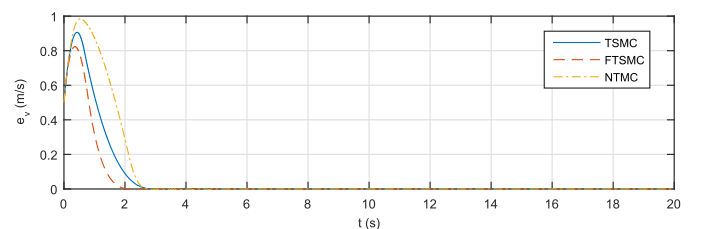


Fig. 9. The velocity tracking errors of the AUV versus time using the proposed control schemes for a circular path.

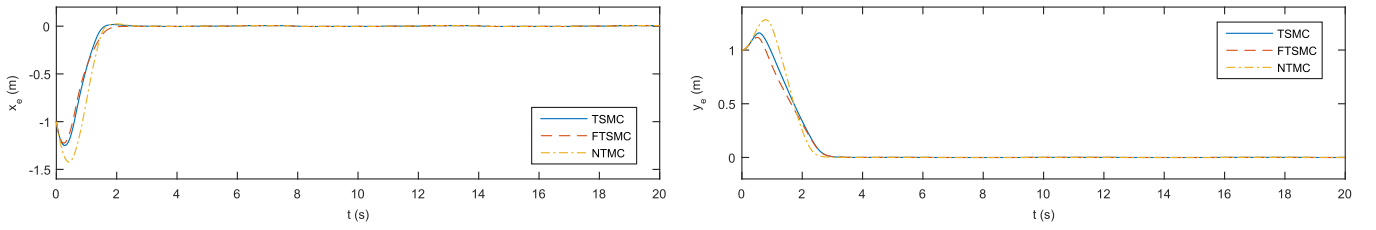


Fig. 10. The position tracking errors of the AUV versus time using the proposed control schemes for a circular path.

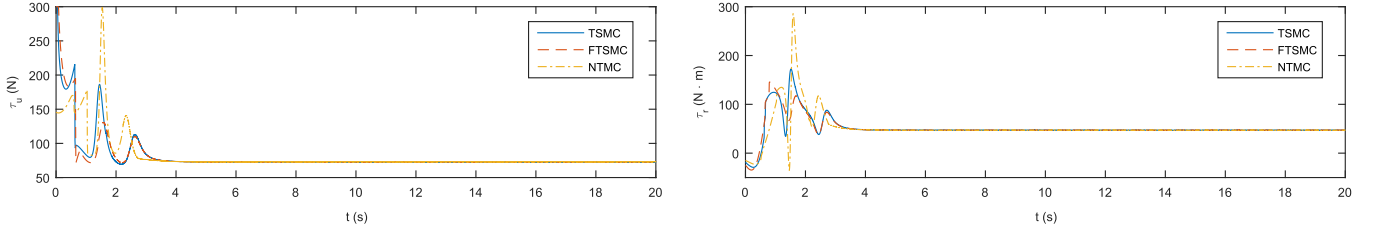


Fig. 11. The surge and yaw controllers of the AUV versus time using the proposed control schemes for a circular path.

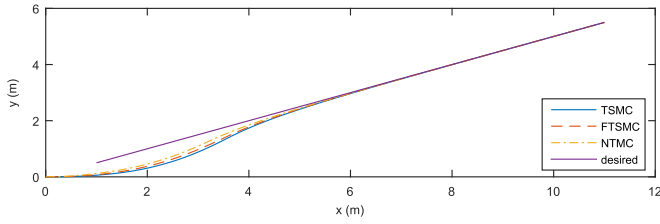


Fig. 12. The actual and desired paths of the AUV using the proposed control schemes with constant disturbances.

and $W_2 = 0.25$.

- NTSMC: $c_1 = 0.5$, $c_2 = 0.3$, $q_1/p_1 = q_2/p_2 = 3/5$, $W_1 = 1.4$ and $W_2 = 1$.

Figs. 3–7 show the simulation results using the three proposed controllers. In Fig. 3, the actual path of the AUV is shown along with the desired one where a good tracking is achieved. The coordinates of the AUV's position, the orientation and the velocities of the AUV versus time are shown in Fig. 4. The boundedness of the velocities is obvious

from this figure. The finite-time convergence of the velocity tracking errors of the AUV to zero is illustrated in Fig. 5. From this figure, it can be noticed that the three controllers manage to force the sliding surface S_1 to reach zero in about 0.9 s using the NTSMC and 1.5 s using the TSMC and FTSMC. Once S_1 reaches zero, the surge velocity error starts converging to zero in finite-time (about 0.5 s, 0.25 s and 0.6 s for TSMC, FTSMC and NTSMC respectively). As for the second sliding surface S_2 , it is forced to reach zero in about 5.2 s using the TSMC and FTSMC and 4.1 s using the NTSMC. Then, the sway velocity error converges to zero in finite time (around 0.4 s, 0.3 s and 0.4 s for TSMC, FTSMC and NTSMC respectively). These results verify the formulas presented in (A.4) and (A.7) for the convergence time. Since the proposed TSM and FTSM controllers impose the dynamics $\dot{S} = -W_i \text{sign}(S_i)$ for ($i = 1, 2$) on the system, the reaching time for the surfaces can be determined using the following equation,

$$t_{r,i} = |S_i(0)|/W_i. \quad (60)$$

Using the initial values, $S_1(0)$ is obtained from (19) and (34) such that $S_1(0) = -0.75$ and $S_1(0) = -0.7$ for the TSM and FTSM controllers

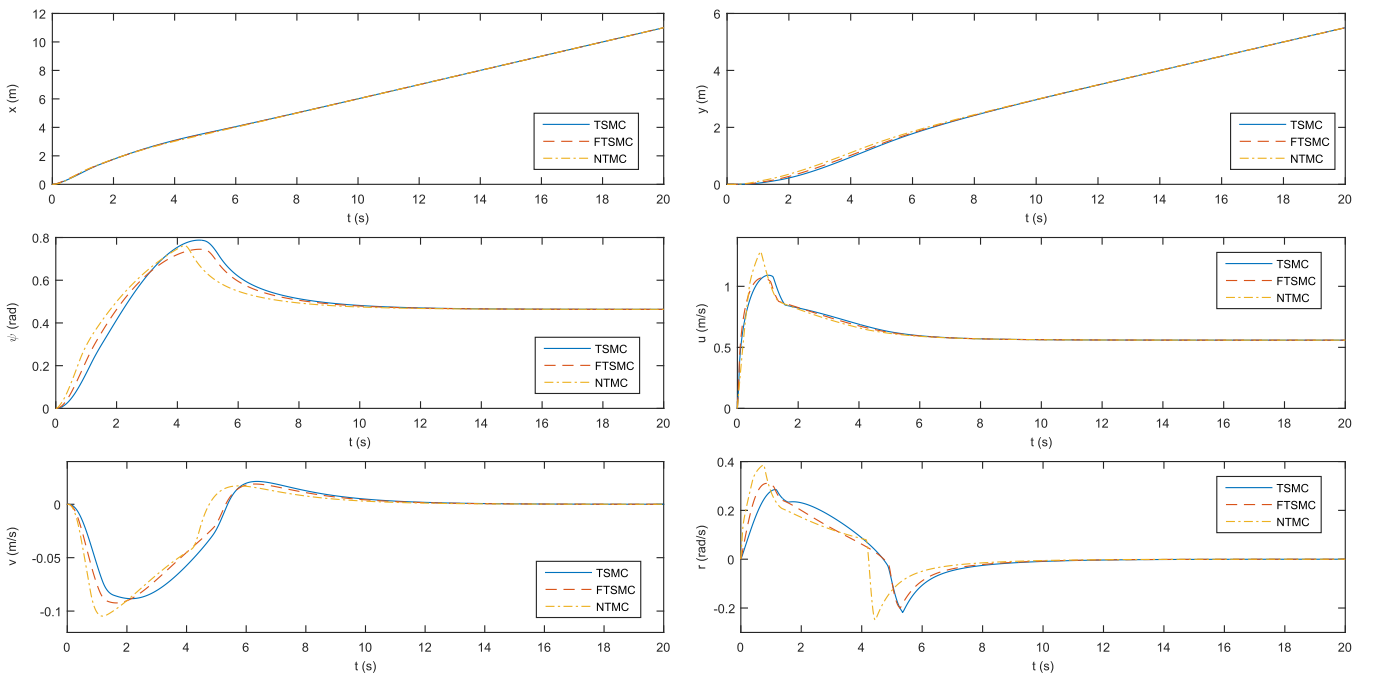


Fig. 13. The positions, the orientation and the velocities of the AUV versus time using the proposed control schemes with constant disturbances.

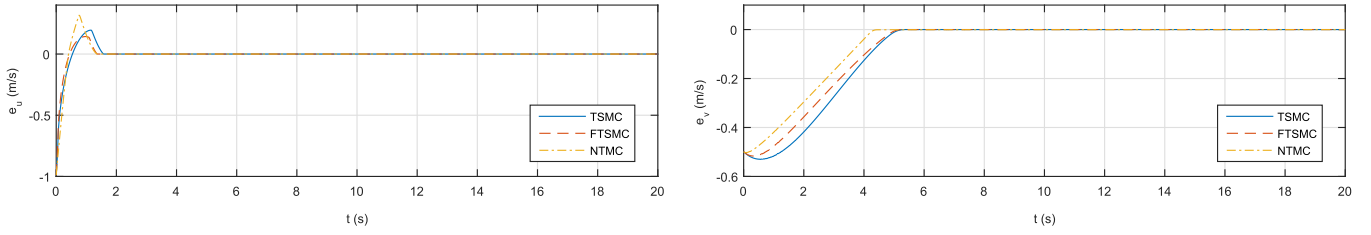


Fig. 14. The velocity errors of the AUV versus time using the proposed control schemes with constant disturbances.

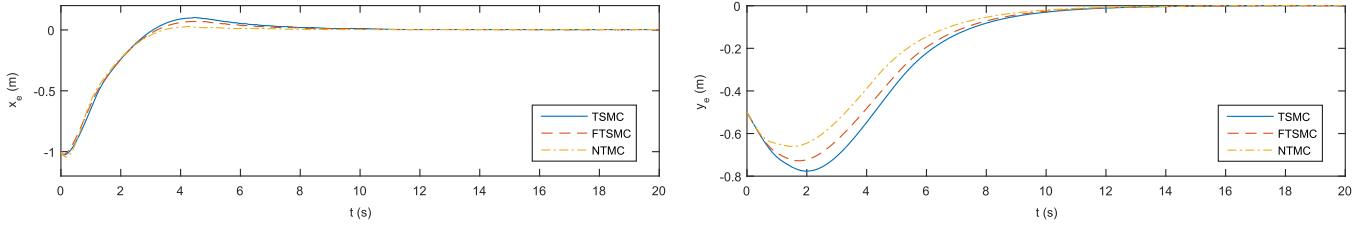


Fig. 15. The position errors of the AUV versus time using the proposed control schemes with constant disturbances.

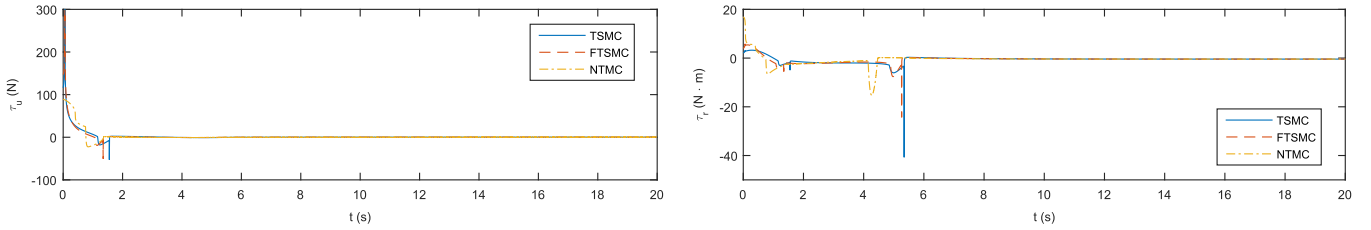


Fig. 16. The surge and yaw controllers of the AUV versus time using the proposed control schemes with constant disturbances.

respectively. This corresponds to a reaching time of $t_{r,1} = 1.5$ seconds using the TSM controller and $t_{r,1} = 1.4$ seconds using the FTSM controller. Moreover, using the Eqs. (A.4) and (A.7), the convergence time of the surge velocity errors $t_{s,1}$ can be calculated to be $t_{s,1} = 1.9$ s using the TSM controller (where $\tilde{e}_u(t_{r,1}) = -0.02$) and $t_{s,1} = 1.65$ s using the FTSM controller (where $\tilde{e}_u(t_{r,1}) = -0.01$). Since these values agree with the obtained results, the formulas given in (A.4) and (A.7) are verified. It should be mentioned that the reaching time obtained using (60) can be slightly different than the results since the exact sign function is replaced using the boundary layer approximation.

Furthermore, the convergence of the position tracking errors of the AUV to zero can be clearly seen in Fig. 6. The surge and sway controllers versus time for the three proposed control laws are presented in Fig. 7. The discontinuous behavior of the controllers can be observed from this figure when the surfaces change their sign where the surge controller τ_u changes its value rapidly making a spike in about 0.9 s using the NTSMC and 1.5 s using the TSMC and FTSMC. As for the yaw controller τ_r , it can be noticed that it changes its value rapidly twice at different time instants for each controller. The first change occurs when the first surface S_1 changes its sign affecting the surge controller, and the second change occurs when S_2 changes its value. This amount of change for each controller is governed by the controllers gains W_1 and W_2 . Consequently, these discontinuous

changes cause the velocities to change in a similar way as can be seen from the results. For practical considerations, the gains of the controllers and the thickness of the boundary layer can be selected properly depending on the ability of the actuators in providing such changes and how fast they can change.

Additionally, more simulations are performed considering a circular motion tracking in order to show the performance of the proposed control schemes with different types of paths. The obtained results for the circular motion are presented in Figs. 8–11. The desired path to be tracked is chosen such that $x_d = 2 \cos(t) - 3$ and $y_d = 2 \sin(t) + 1$. Figs. 8 and 10 show that the circular motion tracking is achieved using the proposed controllers.

The presented results clearly indicate that the proposed control schemes work well for the trajectory tracking of AUVs moving in the horizontal plane.

6. Robustness studies

Simulation studies are presented in this section in order to test the robustness of the proposed control schemes to bounded environmental disturbances, unmodeled dynamics and model uncertainties. To this end, their effects are included in the AUV model described by Eqs. (1) and (2). The effects of environmental disturbances, unmodeled dynamics and model uncertainties are regarded as disturbances, and the new AUV kinematic and dynamic equations including these disturbances are,

$$\begin{aligned} \dot{x} &= u \cos \psi - v \sin \psi \dot{\psi} = u \sin \psi + v \cos \psi \dot{\psi} = r \dot{\psi} = M_1(X_u u + a_{26}vr + \tau_u) + d_1(t) \dot{v} \\ &= M_2(Y_v v + a_{16}ur) \dot{r} = M_6(N_r r + a_{12}uv + \tau_r) + d_2(t) \end{aligned} \quad (61)$$

where the terms d_1 and d_2 represent the disturbances due to environmental disturbances, unmodeled dynamics and model uncertainties. It is assumed that the bounds on d_1 and d_2 are known (or estimated) so that the gains of the controllers can be selected properly in order to suppress the effects of the disturbances. This assumption is valid for

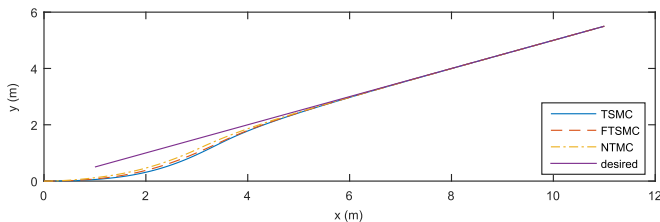


Fig. 17. The actual and desired paths of the AUV using the proposed control schemes with sinusoidal disturbances.

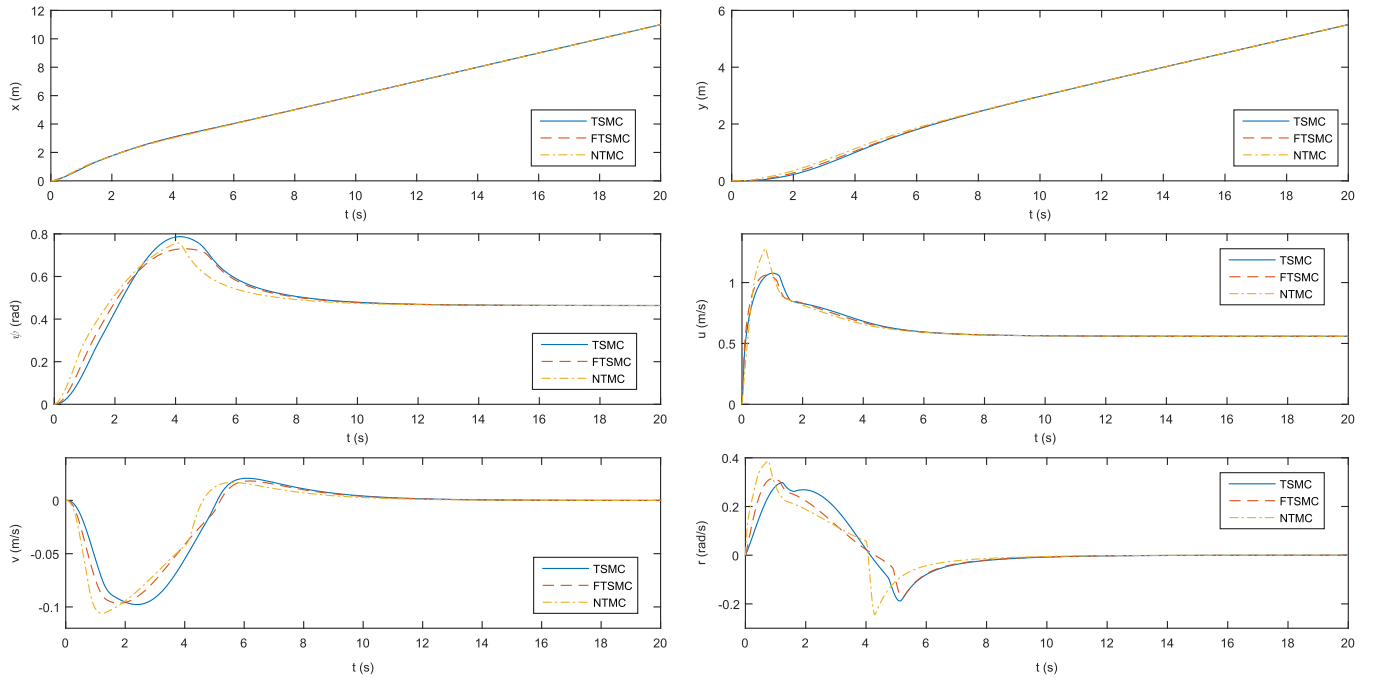


Fig. 18. The positions, the orientation and the velocities of the AUV versus time using the proposed control schemes with sinusoidal disturbances.

many practical environmental disturbances such as wind disturbances, wave disturbances, ocean currents, etc (Fischer et al., 2014; Fossen, 2011; Fang et al., 2006; Moreira and Soares, 2008). Moreover, one can define upper bounds on the unknown terms $d_1(t)$ and $d_5(t)$ based on the structural or measurable knowledge of them (Fischer et al., 2014).

Simulations are performed using the proposed controllers considering different scenarios of disturbances which are as follows,

1. Constant Disturbances,

$$d_1(t) = 0.15, \quad d_2(t) = 0.05 \quad (62)$$

2. Sinusoidal Disturbances,

$$d_1(t) = 0.15 \cos(t), \quad d_2(t) = 0.1 \sin(t) \quad (63)$$

3. Disturbances for a period of time,

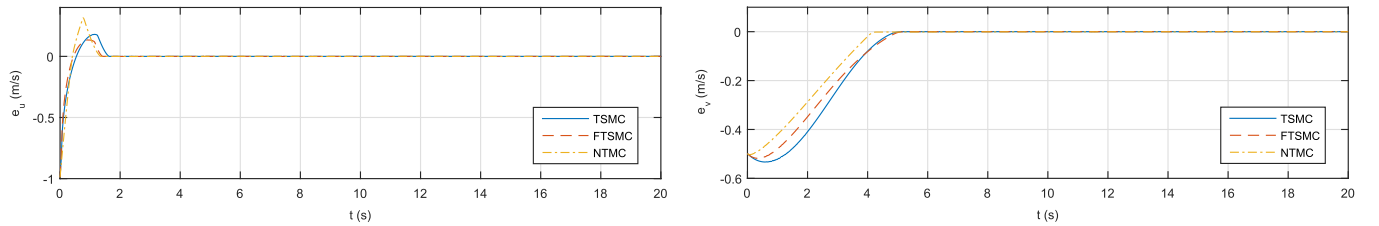


Fig. 19. The velocity errors of the AUV versus time using the proposed control schemes with sinusoidal disturbances.

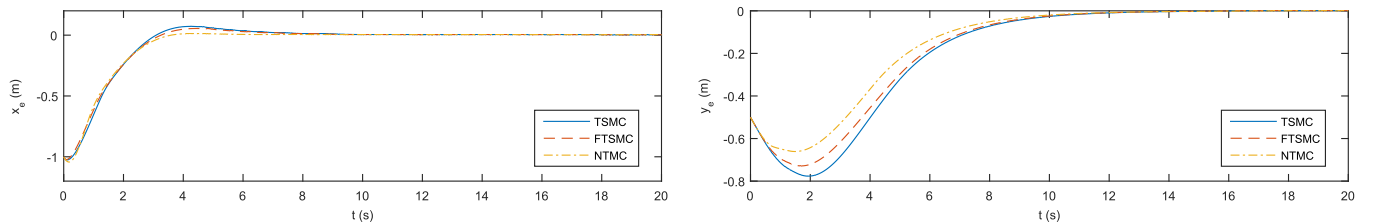


Fig. 20. The position errors of the AUV versus time using the proposed control schemes with sinusoidal disturbances.

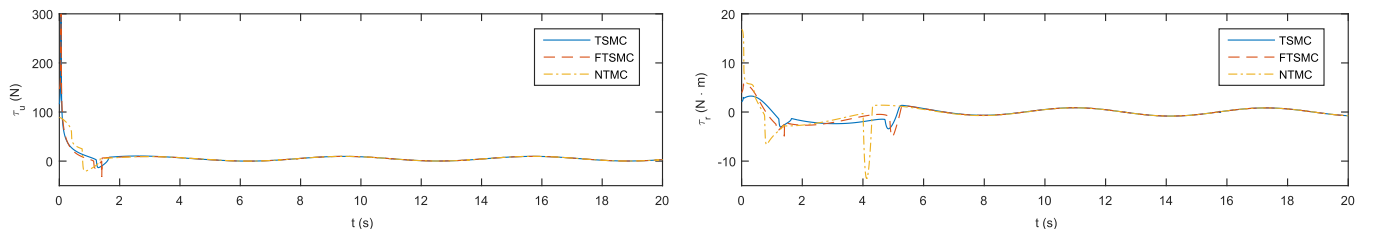


Fig. 21. The surge and yaw controllers of the AUV versus time using the proposed control schemes with sinusoidal disturbances.

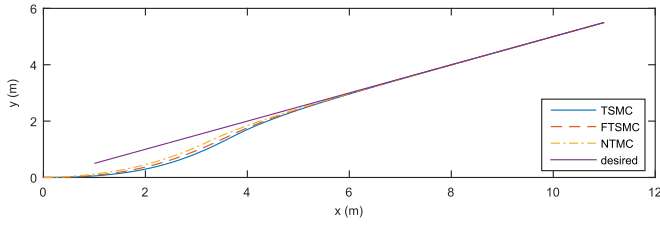


Fig. 22. The actual and desired paths of the AUV using the proposed control schemes with disturbances for a period of time.

$$d_1(t) = 1.5[u_s(t - 10) - u_s(t - 11)], d_2(t) = 0.1[u_s(t - 10) - u_s(t - 11)] \quad (64)$$

where $u_s(t)$ is a unit step function defined as,

$$u_s(t) = \begin{cases} 1, & t \geq 0 \\ 0, & \text{otherwise} \end{cases}$$

Figs. 12–26 show the obtained results from these simulations for the three cases of disturbances; The coordinates of the AUV's position, the orientation and the velocities of the AUV versus time are shown in Figs. 13, 18 and 23, the position errors of the AUV versus time are given in Figs. 15, 20 and 25, the velocity errors of the AUV versus time are shown in Figs. 14, 19 and 24, and the controllers versus time are given in Figs. 16, 21 and 26. It can be seen that the controllers have different values at steady state managing to suppress the effect of the

acting disturbances. For the sinusoidal case, the controllers at steady state update their values in a sinusoidal form. For the third case, once the disturbances act on the vehicle for the period between 10 s and 11 s, the control schemes start to change the values of the required surge force and yaw moment in order to suppress the effect of the disturbances and brings the vehicle back to its path. This case shows the ability of the system to recovers from such disturbances using the proposed control schemes.

We can conclude from these results that the proposed control schemes force the position and velocity errors of the AUV to converge to zero even though there are disturbances acting on the AUV. Therefore, it can be concluded that the proposed control schemes are robust under bounded disturbances.

7. Conclusion

Trajectory tracking control schemes are proposed for the control of the lateral motion of AUVs using the concepts of terminal sliding mode. These controllers aim to force the position of the AUV to track a desired, time-varying trajectory. Each control design is validated by simulating their performances where they are applied to an example AUV. The obtained simulation results indicate that the proposed control schemes solve the trajectory tracking problem for the lateral motion of AUVs. Moreover, some simulation studies are presented to show that these control schemes are robust to bounded disturbances.

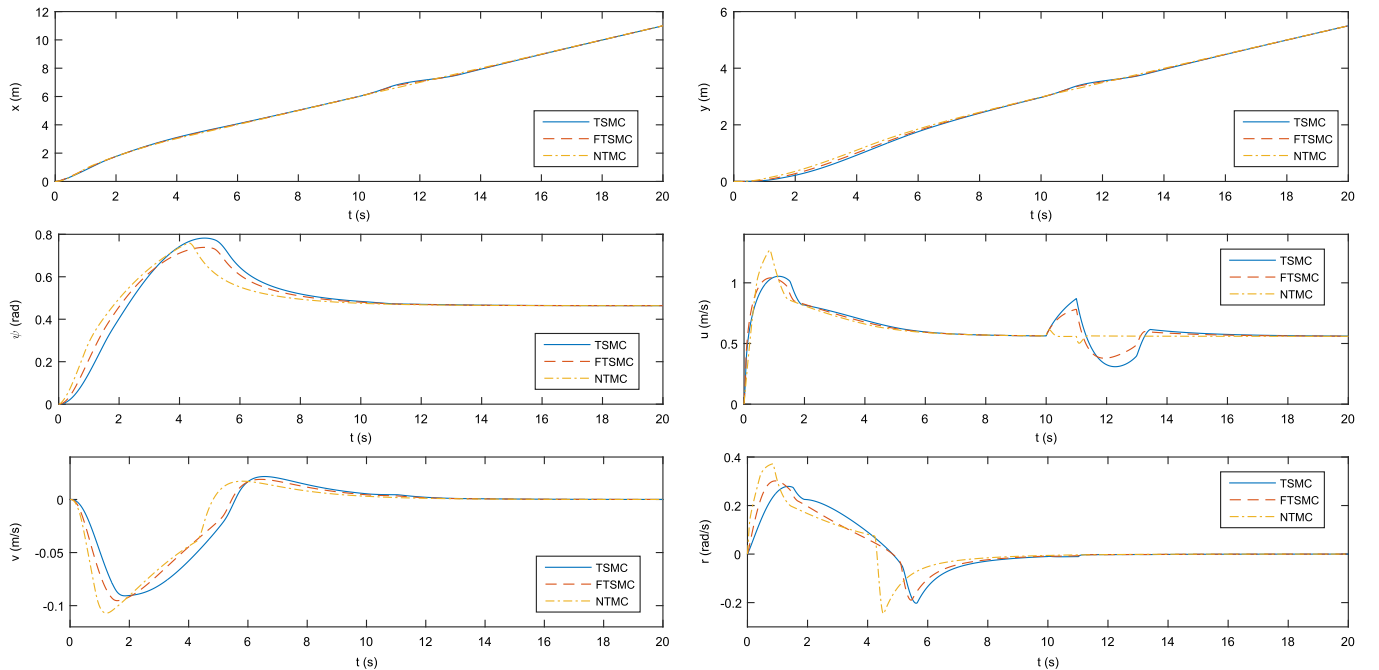


Fig. 23. The positions, the orientation and the velocities of the AUV versus time using the proposed control schemes with disturbances for a period of time.

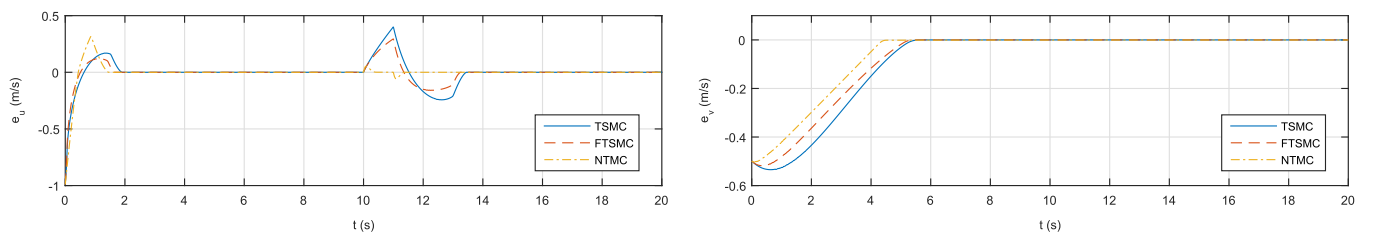


Fig. 24. The velocity errors of the AUV versus time using the proposed control schemes with disturbances for a period of time.

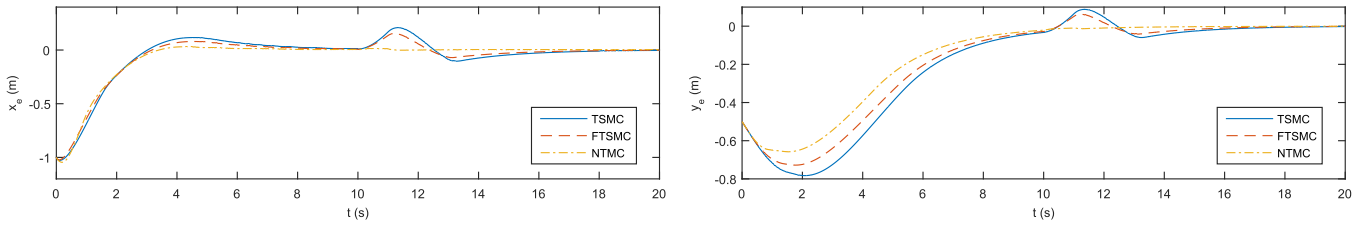


Fig. 25. The position errors of the AUV versus time using the proposed control schemes with disturbances for a period of time.

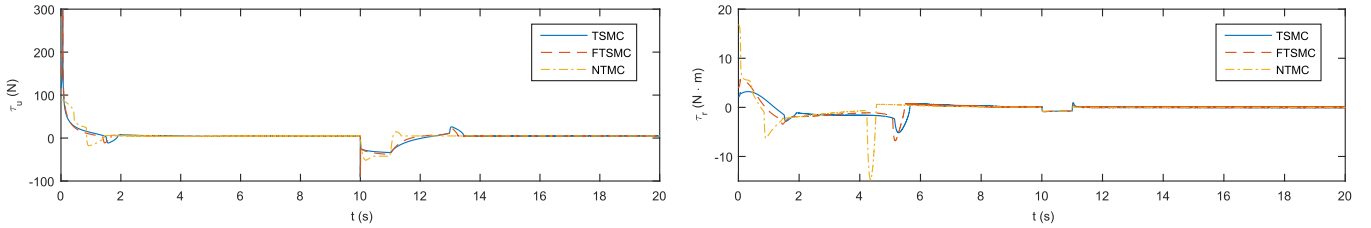


Fig. 26. The surge and yaw controllers of the AUV versus time using the proposed control schemes with disturbances for a period of time.

Acknowledgments

We would like to acknowledge the financial support of the Kuwait

Foundation for the Advancement of Science (KFAS) for the project KFAS 2013–5505-01 (Kuwait-MIT Center).

Appendix A. An overview of terminal sliding mode control

A brief summary of the concepts of terminal sliding mode control is provided here.

Definition 1. (Feng et al., 2002) Consider the following second-order nonlinear system with uncertainties:

$$\dot{x}_1 = x_2, \dot{x}_2 = f(x) + b(x)u + d(x) \quad (\text{A.1})$$

where $x = [x_1, x_2]^T$ represents the states vector of the system, $f(x)$ and $b(x)$ are smooth nonlinear functions such that $b(x) \neq 0$, u is the control input and $d(x)$ is a bounded function that represents the disturbances and model uncertainties such that $|d(x)| \leq D$ with $D > 0$. The terminal sliding mode (TSM) of such a system can be described using one of the following equivalent TSM surface (manifold) forms:

$$S = x_2 + \beta x_1^{q/p} \quad (\text{A.2})$$

$$S = x_2 + \beta |x_1|^{\gamma} \text{sign}(x_1) \quad (\text{A.3})$$

where β is a positive constant, $0 < \gamma < 1$ and p and q are positive odd integers satisfying the condition $p > q$.

The controller u of system (A.1) can be designed to drive the terminal sliding surfaces (A.2) or (A.3) to zero in finite time (i.e. $S=0$). Once there, the dynamics of the system become $\dot{x}_1 = -\beta x_1^{q/p}$ or $\dot{x}_1 = -\beta |x_1|^{\gamma} \text{sign}(x_1)$. This system has a terminal attractor at $x_1 = 0$ which has been shown in (Zak, 1988) and (Zak, 1989). This mean that the finite time convergence of x_1 to zero is guaranteed on the terminal sliding surface in (A.2) and (A.3).

The TSM surfaces described by (A.2) and (A.6) do not differ from each other in terms of the finite-time convergence and the steady-state tracking precision if the design parameters β , p , q and γ are chosen properly.

Lemma 1. (Feng et al., 2002) The equilibrium point $(x_1, x_2) = (0, 0)$ of the system (A.1) is globally finite-time stable on the sliding surface $S=0$ defined by (A.2), [i.e., starting from any initial point $(x_1(0), x_2(0))$, the system states converge to $(x_1, x_2) = (0, 0)$ in finite time t_s and remain there for $t \geq t_s$]. This finite time can be determined using the following equation:

$$t_s = t_r + \frac{p}{\beta(p-q)} [x_1(t_r)]^{\frac{p-q}{p}} \quad (\text{A.4})$$

where t_r is the reaching time, the time taken by the trajectories to reach $S=0$.

When using the dynamics imposed by the TSM surfaces in (A.2) and (A.3), it is noticed that the convergence rate is faster when the trajectories start closer to the equilibrium resulting in finite time convergence. On the other hand, when the states of the system are far away from the equilibrium point, the TSM is not superior to the conventional sliding mode control (SMC) because of the terms $(x_1)^{q/p}$ and $|x_1|^{\gamma}$; these terms reduce the convergence rates at a distance far from the equilibrium since the powers are less than one. Therefore, a solution was proposed in (Yu et al., 1999) through the introduction of the so-called fast terminal sliding mode (FTSM).

Definition 2. (Yu et al., 1999; Yu and Zhihong, 2002) For the system (A.1), the FTSM can be described by one of the following nonlinear surfaces:

$$S = x_2 + \alpha x_1 + \beta (x_1)^{q/p} \quad (\text{A.5})$$

$$S = x_2 + \alpha x_1 + \beta |x_1|^{\gamma} \text{sign}(x_1) \quad (\text{A.6})$$

where $\alpha, \beta > 0$, $0 < \gamma < 1$, and p and q are positive odd integers such that $p > q$.

Lemma 2. (Yu and Zhihong, 2002) *On the sliding surface $S=0$ where S is defined in (A.5), the equilibrium point $(x_1, x_2) = (0, 0)$ of the system (A.1) is globally finite-time stable with a settling time t_s such that:*

$$t_s = t_r + \frac{p}{\alpha(p-q)} \ln \frac{\alpha(x_1(t_r))^{\frac{p-q}{p}} + \beta}{\beta} \quad (\text{A.7})$$

where t_r is the reaching time, the time taken by the trajectories to reach $S=0$. Eq. (A.7) indicates faster finite-time stability when compared with the TSM settling time in (A.4).

The physical interpretation of Lemma 2 is such that when the state x_1 is far from the origin, the dynamics of (A.5) can be approximated as: $\dot{x}_1 = -\alpha x_1$ which leads to fast convergence when far away from zero. When x_1 is close to the origin, the dynamics can be approximated as: $\dot{x}_1 = -\beta x_1^{q/p}$ which is a terminal attractor.

References

- Antonelli, G., Caccavale, F., Chiaverini, S., Fusco, G., 2003. A novel adaptive control law for underwater vehicles. *IEEE Trans. Control Syst. Technol.* 11, 221–232.
- Ashrafiuon, H., Muske, K.R., McNinch, L.C., Soltan, R.A., 2008. Sliding-mode tracking control of surface vessels. *IEEE Trans. Ind. Electron.* 55, 4004–4012.
- De Jager, B., 1992. Comparison of methods to eliminate chattering and avoid steady state errors in sliding mode digital control. In: *Proceedings of the IEEE VSC and Lyapunov Workshop*, Sheffield, pp. 37–42.
- Do, K., Pan, J., Jiang, Z., 2004. Robust and adaptive path following for underactuated autonomous underwater vehicles. *Ocean Eng.* 31, 1967–1997.
- Fang, M.C., Chang, P.E., Luo, J.H., 2006. Wave effects on ascending and descending motions of the autonomous underwater vehicle. *Ocean Eng.* 33 (14), 1972–1999.
- Feng, Y., Yu, X., Man, Z., 2002. Non-singular terminal sliding mode control of rigid manipulators. *Automatica* 38, 2159–2167.
- Feng, Y., Yu, X., Han, F., 2013. On nonsingular terminal sliding-mode control of nonlinear systems. *Automatica* 49, 1715–1722.
- Fischer, N., Hughes, D., Walters, P., Schwartz, E.M., Dixon, W.E., 2014. Nonlinear RISE-based control of an autonomous underwater vehicle. *IEEE Trans. Robot.* 30 (4), 845–852.
- Fossen, T.I., 2002. Marine control systems guidance, navigation and control of ships, rigs and underwater vehicles. *Mar. Cybern. AS*.
- Fossen, T.I., 2011. *Handbook of marine craft hydrodynamics and motion control*. John Wiley and Sons.
- Fujii, T., Ura, T., 1990. Development of motion control system for AUV using neural nets, In: *Proceedings of the (1990) Symposium on Autonomous Underwater Vehicle Technology*, IEEE, pp. 81–86.
- Geranmehr, B., Nekoo, S.R., 2015. Nonlinear suboptimal control of fully coupled non-affine six-DOF autonomous underwater vehicle using the state-dependent Riccati equation. *Ocean Eng.* 96, 248–257.
- Healey, A.J., Lienard, D., 1993. Multivariable sliding mode control for autonomous diving and steering of unmanned underwater vehicles. *IEEE J. Ocean. Eng.* 18, 327–339.
- Jiang, Z.P., 2002. Global tracking control of underactuated ships by lyapunov's direct method. *Automatica* 38, 301–309.
- Joe, H., Kim, M., Yu, S.c., 2014. Second-order sliding-mode controller for autonomous underwater vehicle in the presence of unknown disturbances. *Nonlinear Dyn.* 78, 183–196.
- Khaled, N., Chalhoub, N.G., 2013. A self-tuning guidance and control system for marine surface vessels. *Nonlinear Dyn.* 73, 897–906.
- Khan, M.K., 2003. *Des. Appl. Second Order sliding mode Control Algorithms*, (Dr. Diss., Eng.).
- Lefeber, E., Pettersen, K.Y., Nijmeijer, H., 2003. Tracking control of an underactuated ship. *IEEE Trans. Control Syst. Technol.* 11, 52–61.
- Li, J.H., Lee, P.M., 2005. Design of an adaptive nonlinear controller for depth control of an autonomous underwater vehicle. *Ocean Eng.* 32, 2165–2181.
- Martins, F.N., Celeste, W.C., Carelli, R., Sarcinelli-Filho, M., Bastos-Filho, T.F., 2008. An adaptive dynamic controller for autonomous mobile robot trajectory tracking. *Control Eng. Pract.* 16, 1354–1363.
- McGann, C., Py, F., Rajan, K., Ryan, J.P., Henthorn, R., 2008. Adaptive control for autonomous underwater vehicles. In: *Proceedings of the 23rd National Conference on Artificial Intelligence-Volume 3*, pp. 1319–1324.
- Moreira, L., Soares, C.G., 2008. H_2 and H_∞ designs for diving and course control of an autonomous underwater vehicle in presence of waves. *IEEE J. Ocean. Eng.* 33 (2), 69–88.
- Neila, M.B.R., Tarak, D., 2011. Adaptive terminal sliding mode control for rigid robotic manipulators. *Int. J. Autom. Comput.* 8, 215–220.
- Pettersen, K.Y., Nijmeijer, H., 2001. Underactuated ship tracking control theory and experiments. *Int. J. Control* 74, 1435–1446.
- Qi, X., 2014. Adaptive coordinated tracking control of multiple autonomous underwater vehicles. *Ocean Eng.* 91, 84–90.
- Repoulas, F., Papadopoulos, E., 2007. Planar trajectory planning and tracking control design for underactuated AUVs. *Ocean Eng.* 34 (11–12), 1650–1667.
- Sahu, B.K., Subudhi, B., 2014. Adaptive tracking control of an autonomous underwater vehicle. *Int. J. Autom. Comput.* 11, 299–307.
- Wang, H., Wang, D., Peng, Z., 2014. Adaptive dynamic surface control for cooperative path following of marine surface vehicles with input saturation. *Nonlinear Dyn.* 77, 107–117.
- Wang, J., Sun, Z., 2012. 6-DOF robust adaptive terminal sliding mode control for spacecraft formation flying. *Acta Astronaut.* 73, 76–87.
- Wang, J.S., Lee, C.G., 2003. Self-adaptive recurrent neuro-fuzzy control of an autonomous underwater vehicle. *IEEE Trans. Robot. Autom.* 19, 283–295.
- Wang, L., Jia, H.m., Zhang, L.j., Wang, H.b., 2012. Horizontal tracking control for AUV based on nonlinear sliding mode. In: *Proceedings of the International Conference on Information and Automation (ICIA)*, IEEE, pp. 460–463.
- Yoerger, D.R., Slotine, J.J., 1985. Robust trajectory control of underwater vehicles. *IEEE J. Ocean. Eng.* 10, 462–470.
- Yu, R., Zhu, Q., Xia, G., Liu, Z., 2012. Sliding mode tracking control of an underactuated surface vessel. *IET Control Theory Appl.* 6, 461–466.
- Yu, X.H., Zhihong, M., 2002. Fast terminal sliding-mode control design for nonlinear dynamical systems. *IEEE Circuits Syst. Soc.* 49, 261–264.
- Yu, X., Wu, Y., Zhihong, M., 1999. On global stabilization of nonlinear dynamical systems. In: *Variable Structure Systems, Sliding Mode and Nonlinear Control*. Springer, pp. 109–122.
- Yuh, J., 1990. A neural net controller for underwater robotic vehicles. *IEEE J. Ocean. Eng.* 15, 161–166.
- Yuh, J., 1994. Learning control for underwater robotic vehicles. *IEEE Control Syst.* 14, 39–46.
- Zak, M., 1988. Terminal attractors for addressable memory in neural networks. *Phys. Lett. A* 133 (1), 18–22.
- Zak, M., 1989. Terminal attractors in neural networks. *Neural Netw.* 2 (4), 259–274.
- Zou, A.M., Kumar, K.D., Hou, Z.G., Liu, X., 2011. Finite-time attitude tracking control for spacecraft using terminal sliding mode and Chebyshev neural network. *IEEE Trans. Syst., Man, Cybern., Part B: 390 Cybern.* 41, 950–963.